IET-UK International Conference on Information and Communication Technology in Electrical Sciences (ICTES 2007), Dr. M.G.R. University, Chennai, Tamil Nadu, India. Dec. 20-22, 2007. pp.69-74.

A CLOSED LOOP STABILITY ANALYSIS FOR THE PARTICLE SWARM OPTIMIZATION DYNAMICS

Debadeep Sen, Siladitya Dey

ETCE Department, Jadavpur University, Kolkata, India
Email: debadeep.sen@gmail.com, dey.siladitya@gmail.com

Abstract

The paper presents an alternative formulation of the PSO dynamics by a closed loop Control System, and analyzes the stability behavior of the system by using Jury's test and root locus technique. Previous stability analysis of the PSO dynamics was restricted because of no explicit modeling of the non-linear element in the feedback path. In the present analysis, the model of the non linear element is considered for closed loop stability analysis. Unlike the previous works on stability analysis, where the acceleration coefficients have been combined into a single term, we in this paper consider their separate existence to determine their suitable range to ensure stability of the dynamics. The range of parameters of the PSO dynamics, obtained by Jury's test and root locus technique are also confirmed by computer simulation of the PSO algorithm.

1 Introduction

Pioneered by Eberhart and Kennedy, the Particle Swarm Optimization(PSO) algorithm is a population based intelligent search, where individuals called particles are candidate solutions to the given optimization problem. In a PSO algorithm, particles adapt their velocities and positions in each iteration to search the optima in a multidimensional space until one or more particles converge to the global optima. Currently, the PSO dynamics is modeled by a feedback control system, where the forward path represents the dynamics of an individual particle and the feedback path includes a non-linear element. Unfortunately existing stability analysis of PSO dynamics is restricted, because of the absence of a suitable representation of the non-linear element in the feedback path [3], [4]. In this paper, we consider possible representation of the non-linear element and perform the stability analysis of the closed loop system using Jury's test [6] and root-locus technique [7], [8].

In this paper, we propose closed loop stability analysis of the PSO dynamics. The analysis differs from the existing works [1], [13] by the following counts. Unlike the previous works, we here explicitly represent the non-linear element by mathematical models and perform the stability analysis for the closed loop system using this model. The analysis, unlike the previous works, considers the separate existence of the acceleration coefficients, and determines their range for stability analysis. Further, the state-space representation of the PSO dynamics here has been built in order to i) minimize the positional shift of a particle from the global best position, so far determined, and ii) command the PSO dynamics with the error between the global and local best positions of the particle. This idea is classically different, and helps in simplifying the analysis even when the global best position is not known explicitly.

The non-linear element here has been modeled to yield the local best position at time t by considering its previous value and the current position of the particle. Jury's test has been applied on the characteristic equation of the closed loop system to determine the conditions for stability for the closed loop dynamics. These conditions reveal suitable range of parameters for the PSO dynamics, and are also supported by the established results. The root locus analysis for the closed loop system provides finer ranges for the acceleration coefficients that satisfy the stability conditions for two possible representations of the non-linear element. Computer simulation of the PSO algorithm also supports the results of stability analysis.

The paper is organized as follows. The basic PSO algorithm and its state space analysis are under taken in Section 2. The closed loop representation of the PSO dynamics and modeling of the non-linear element is considered in section 3. Stability analysis by Jury's test is performed in section 4. Parameter selection for the PSO dynamics by root locus technique is undertaken in section 5. Computer simulations supporting the established result of section 5 are given in section 6. Conclusions are listed in section 7.

2 The PSO Dynamics and Its State Space Representation

The PSO dynamics usually is represented in a d-dimensional space with a memory of its previous best position and global best position among all particles. The particle position at time t is equivalent from its previous position at time (t-1) and current velocity. The current velocity is also adapted from its previous velocity, difference of the particle position from its local best position and difference from global best position. For convenience of the analysis we consider one dimensional particle dynamics for the PSO as follows.

$$v_t = \omega . v_{t-1} + \alpha^l_{(t-1)} (p^l - x_{t-1}) + \alpha^g_{(t-1)} (p^g - x_{t-1}) \quad \text{........(1)}$$

$$x_t = x_{t-1} + v_t \quad \text{..(2)}$$

where v_t is the velocity of the particle at t^{th} iteration, x_t is the particle position at the t^{th} iteration, pl is the personal (local) best position of the particle so far achieved, pg is the global best position among all particles. The parameters in the PSO dynamics that we need to determine for stability analysis include the inertia factor, the acceleration coefficients for the local best α_t^l and that for the global best position α_t^g. Following the classical analysis and empirical simulation results, we know ω, α^l and α^g all are >0 and α^g and α^g are positive and bounded random numbers.

Let,

$$\bar{x}_t = p^g - x_t$$

Hence, $p^l - x_t = p^l + (\bar{x}_t - p^g)$

$$= (p^l - p^g) + \bar{x}_t \quad (3)$$

$$v_t = \omega . v_{t-1} + \alpha_{t-1} . \bar{x}_{t-1} + \alpha^l_{t-1} (p^l - p^g)$$

Where

$\alpha_{t-1} = \alpha^l_{t-1} + \alpha^g_{t-1}$

Further,

$$\bar{x}_t = p^g - x_t$$

$$= p^g - x_{t-1} - v_t \quad (5)$$

$$= p^g - x_{t-1} - \omega v_{t-1} - \alpha_{t-1} . \bar{x}_{t-1} - \alpha^l_{t-1} (p^l - \alpha^g) \quad (6)$$

[by substitution of (4)]

$$= (1 - \alpha_{t-1}) . \bar{x}_{t-1} - \omega v_{t-1} - \alpha^l_{t-1} (p^l - p^g) \quad (7)$$

Representing equations (4) and (7) in vector matrix form we obtain,

$$\begin{pmatrix} \bar{x}_t \\ v_t \end{pmatrix} = \begin{pmatrix} (1 - \alpha_{t-1}) & -\omega \\ \alpha_{t-1} & \omega \end{pmatrix} \begin{pmatrix} \bar{x}_{t-1} \\ v_{t-1} \end{pmatrix} + \begin{pmatrix} -\alpha^l_{t-1} \\ \alpha^l_{t-1} \end{pmatrix} . (p^l \quad - p^g) \quad (8)$$

This is the state equation for basic PSO algorithms. Here,

is the system matrix.

$$A = \begin{pmatrix} (1 - \alpha_{t-1}) & -\omega \\ \alpha_{t-1} & \omega \end{pmatrix}$$

The stability of the system dynamics can be envisaged from the eigen values (λ) of the above matrix.

Setting det(A – λI) = 0, we obtain

$$\lambda = \frac{(1 - \alpha_{t-1} + \omega) \pm \sqrt{(1 - \alpha_{t-1} - \omega)^2 - 4\omega}}{2}$$

Defining $\alpha_{t-1} - \omega - 1 = \delta$ (9)

$$\lambda = \frac{-\delta \pm \sqrt{\delta^2 - 4\omega}}{2} \quad (10)$$

3 Closed Loop Representation of the PSO Dynamics

Stability of the dynamics now can be ascertained from the eigen values of the above system. The state equation (8) can be described in terms of feedback Control System model as outlined in Fig.1

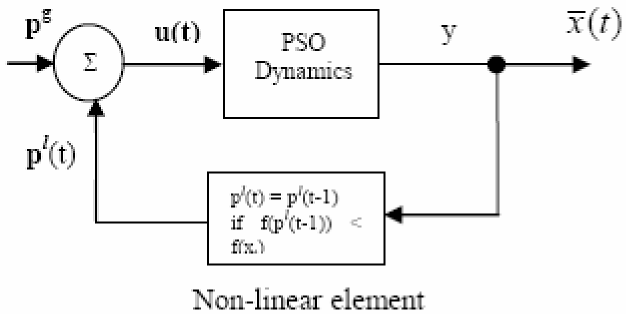

Figure 1: The feedback control representation of particle dynamics

Here the non-linear element determines p^l_t from its previous value p^l_{t-1} and x_t. The non-linear function formally represented by

$p^l_t = p^l_{t-1}$ if $f(p^l_t) < f(x_t)$

$= x_t$, otherwise

where f(.) denotes the fitness function of the rough non-linear search space.

The PSO dynamics being linear can be represented in the form of a transfer function,

Let,

$$M(Z) = \frac{Y(Z)}{U(Z)}$$

Since the state equation consists of two variables $\bar{x}_t$ and v_t and we are interested to feedback $\bar{x}_t$ only, we select a matrix C = [1 0].

The output equation is given by

$$Y = C \tag{11}$$

The M(Z) can be evaluated by

$C(ZI - A)^{-1}B$

$$= \frac{1}{\Delta}(-z\alpha^l) \tag{12}$$

Where $\Delta = (z-\omega)(z-1+\alpha_{t-1}) + \omega\alpha_{t-1}$

$$= z^2 + z(\alpha_{t-1} - \omega - 1) + \omega \tag{13}$$

$$\text{Thus, } \frac{\bar{x}(z)}{u(z)} = \frac{-z\alpha^l}{z^2 + z(\alpha_{t-1} - \omega - 1) + \omega} \tag{14}$$

The non-linear can be modeled by considering two possible values for p^l_t.

$$p^l_t \leftarrow p^l_{t-1} \text{ for } f(p^l_{t-1}) < f(\bar{x}_t) \tag{15}$$

$$\text{and } p^l_t \leftarrow x_t = p^g - \bar{x}_t \tag{16}$$

The first condition can be modeled by using

$$p^l_t \leftarrow \text{Min}\,\{\bar{x}_t\} \tag{17}$$

Since Min $\{\bar{x}_t\}$ is not known, we presume p^l_t as one of the previous $\bar{x}_t$. Thus we write $p^l_t \leftarrow Z^{-n}\,\bar{x}\,(Z),\ n \geq 1$ (18)

The second condition can be written as

$$p^l_t \leftarrow p^g - \bar{x}\,(Z) \tag{19}$$

Based on equation (19) we modify the closed loop configuration of Fig.1, as indicated in Fig. 2(a), The equivalent representation of Fig.2(a) is given in Fig.2(b). The closed loop representation of equation (18) is given in Fig. 3.

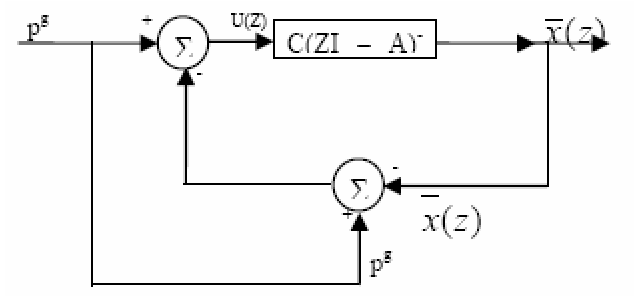

Figure 2(a): Representation of the PSO closed loop dynamics by modeling non-linearity using equation (19).

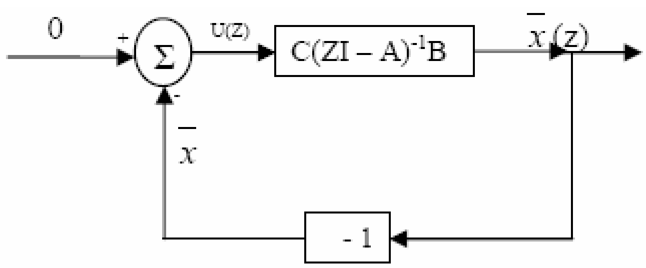

Figure 2(b): An equivalent representation of Fig 2(a).

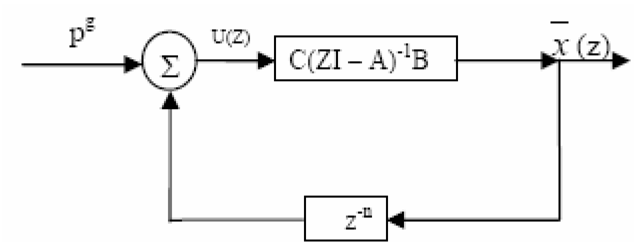

Figure 3: Representation of the PSO closed loop dynamics by modeling nonlinearity using equation (18).

4 Stability Analysis of Closed Loop System

The characteristic equation for the given system vide

Fig.2(b) is given by:

$1 + (-1)\, C(ZI - A)^{-1}B = 0$,

which yields

$F(Z) = 1 + Z^{-1}(\alpha_{t-1} - \omega - 1 - \alpha^{l}_{t-1}) + Z^{-2}\omega = 0$

$\Rightarrow F(Z) = Z^2 + Z(\alpha^{g}_{t-1} - \omega - 1) + \omega$

According to Jury's test,

$F(1) = 1 + (\alpha^{g}_{t-1} - \omega - 1) + \omega > 0$

$\Rightarrow \alpha^{g}_{t-1} > 0$

$F(-1) = 1 - (\alpha^{g}_{t-1} - \omega - 1) + \omega > 0$

$\Rightarrow \alpha^{g}_{t-1} < 2(1+\omega)$ (20)

Further by Jury's test, $|a_0| < a_2$ yields

$\Rightarrow \omega < 1$ (21)

The range of α^{g}_{t-1} as obtained from (20) and (21) is,

$0 < \alpha^{g}_{t-1} < 2(1+\omega)$ for all t.

On the other hand, when we consider the closed loop dynamics

of Fig.3, the characteristic equation is given by,

$F(Z) = 1 + C(ZI - A)^{-1}B.Z^{-1}, n \geq 1$ (22)

$= Z^{n+2} + Z(\alpha^{g}_{t-1} - \omega - 1) + \omega = 0$

Now, by Jury's test $|a_0| < a_{n+2}$ yields $\omega < 1$.

$F(1) > 0$ yields $1 + (\alpha^{g}_{t-1} - \omega - 1) + \omega > 0$

$\Rightarrow \alpha^{g}_{t-1} > 0$ (23)

$F(-1) = -1 - (\alpha^{g}_{t-1} - \omega - 1) + \omega < 0$, for odd (n+2)

$\Rightarrow \alpha^{g}_{t-1} > 2\omega$ (24)

Combining (23) and (24)

$2\omega < \alpha^{g}_{t-1} < 2\omega + 2$ (25)

5 Root Locus Method for Stability Analysis for the PSO Dynamics

For convenience of the analysis, we first consider phase of the G(Z).H(Z) is -1800, where G(Z) is the forward path gain and H(Z) is the feedback path gain.

Setting Z = x + jy, we thus obtain

$$G(Z).H(Z) = \frac{-(x+jy)\alpha^{l}}{(x+jy)^2 + (x+jy)(\alpha_{t-1} - \omega - 1) + \omega} . (-1)$$

$$\angle G(Z).H(Z) = \tan^{-1} y/x - \tan^{-1} \frac{2xy + y(\alpha_{t-1} - \omega - 1)}{x^2 - y^2 + x(\alpha_{t-1} - \omega - 1) + \omega} = -180^0$$

$$\Rightarrow \frac{y}{x} = \frac{2xy + y(\alpha_{t-1} - \omega - 1)}{x^2 - y^2 + x(\alpha_{t-1} - \omega - 1) + \omega}$$

$$\Rightarrow x^2 + y^2 = \omega \quad (26)$$

This is a equation of circle with radius $\sqrt{\omega}$ and centre with (0,0). The breakaway point is obtained by setting

$\frac{d\alpha^{l}}{dz} = 0$, where,

$$\alpha^{l} = \frac{z^2 + z(\alpha_{t-1} - \omega - 1) + \omega}{-z}$$

$$\frac{d\alpha^{l}}{dz} =$$

$$\frac{z(2z + \alpha_{t-1} - \omega - 1) - (z^2 + z(\alpha_{t-1} - \omega - 1) + \omega}{z^2} = 0$$

$$\Rightarrow 2z^2 + z\alpha_{t-1} - z\omega - z - z^2 - z\alpha_{t-1} + z\omega + z - \omega = 0$$

$$\Rightarrow z^2 = \omega$$

$$\Rightarrow z = \sqrt{\omega} \quad (27)$$

It is apparent from equation (26) that the root locus plot for the given transfer function is a circle with centre at origin and radius = ω . A series of root locus plots has been undertaken for different αt-1, the results of which for the two alternative closed loop systems Fig.2(b) and Fig.(3) are presented in Table 1 and 2(a), 2(b) and 2(c) below. It is indicative from the four tables that the PSO dynamics stable for α^{l}_{t-1} in [0,0.013]. Consequently αgt-1 appears to have a range:[0,(4 – 0.103)] = 0,3.877].This is one of the primary achievements of this paper, which to the best of the authors' knowledge can uniquely determine the valuation space for the acceleration coefficients to ensure the stability of the PSO dynamics.

The selection of α^l from the root locus plot was made based on the location of the dominant poles (complex conjugate poles close to the origin [23]). Naturally, the selected value of α^l_{t-1} represents the DC gain of the closed loop system, when it is approximated by the pair of complex conjugate dominant poles. Figure 4(a), 4(b), 4(c) and 4(d) provide a plot of α^l versus ω for constant αt-1 = 1,2 or 3. It is noted from this figure that with increasing ω in the range from 0.1 to 1, α^l decreases monotonically. Fig.5(a), 5(b), 5(c) and 5(d) also reveal that for increasing αt-1 the plots are more or less parallel with higher values of α^g_{t-1}. The root locus plots for stability analysis are subsequently shown in Fig. 6(a), 6(b) and 6(c).

6 Computer Simulation and Results

In this section, we present the results of computer simulation for the basic PSO algorithm outlined in section 2. Computer simulation of the basic PSO algorithm was undertaken on an IBM Pentium machine in C-language under Linux environment. The standard test functions F1 through F10 were used to study the performance of the basic PSO algorithm with the selected parameter range as outlined in this paper. Simulation results confirm that for the selected range of α^l_{t-1} and α^g_{t-1}, PSO converges much earlier with a very good average fitness than the cases when the parameters go outside the range. It is also noted that for the selected range of α^l_{t-1} and α^g_{t-1}, the average fitness increases at a faster rate than the cases where parameters are selected outside this range. Consequently, the simulation reveals that the predicted acceleration coefficients and inertia factor play a significant role in controlling the stabilization behavior of the PSO dynamics.

(The authors regret the lack in clarity of the graphs caused due to space constraints. Interested people may contact the authors for the actual graphs).

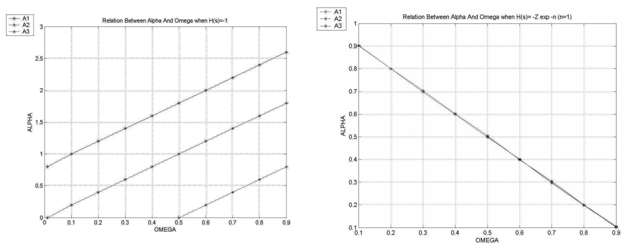

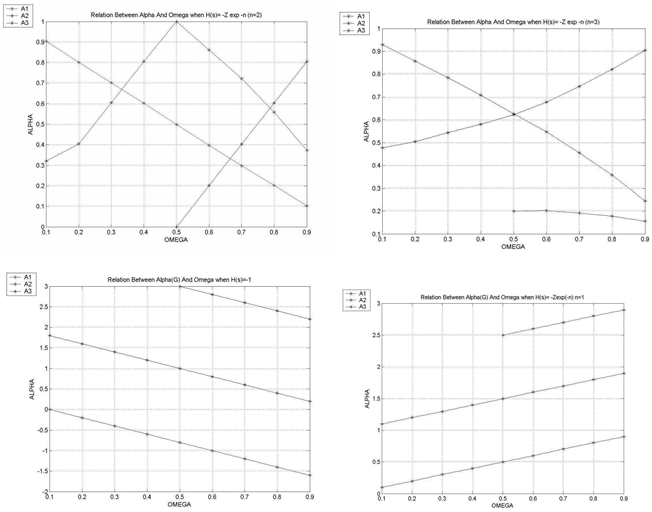

Root Locus Analysis when H(Z) = -1

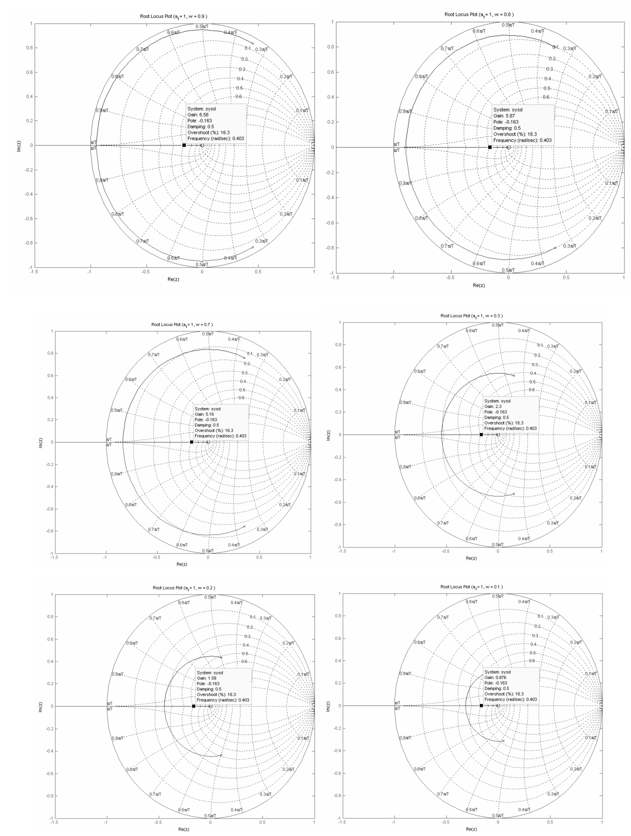

Root Locus analysis for stability when H(Z) = - Z^{-n}, for n = 1

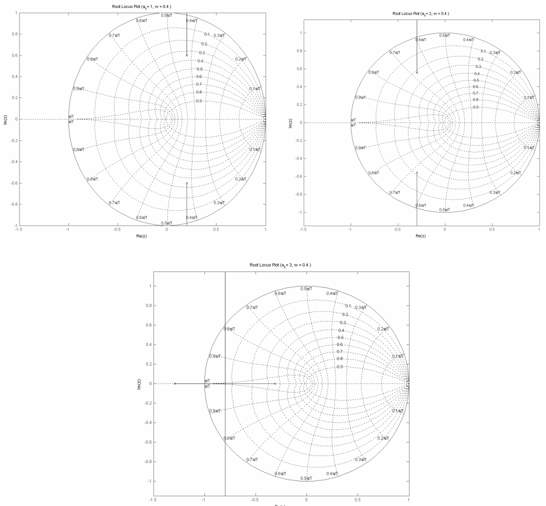

Root Locus analysis for stability when $H(Z) = -Z^{-n}$, for n = 2

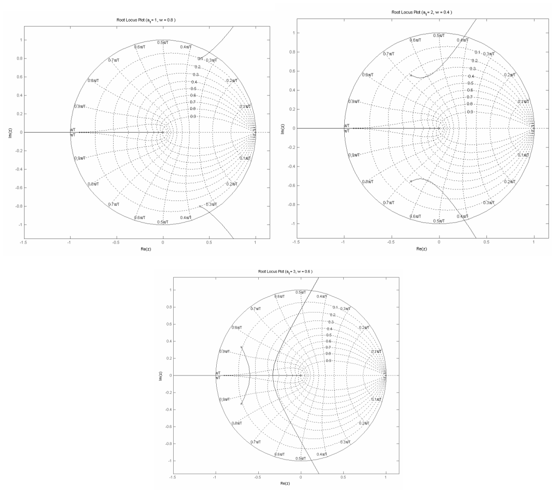

Root Locus analysis for stability when $H(Z) = -Z^{-n}$, for n = 3

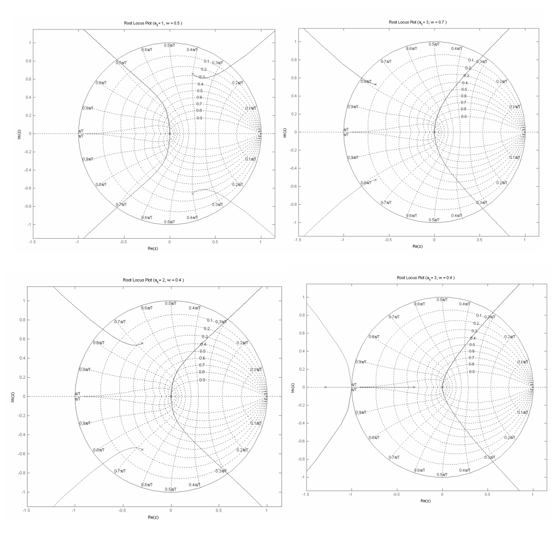

7 Conclusions

The paper proposed a novel approach to closed loop analysis of the PSO dynamics by Jury's test and root locus technique. Jury's stability test confirms established range for the inertia factor (ω), but also provides a new range for the acceleration co-efficient α^{g}_{t-1} in [0, 2(1+ω)]. The root locus analysis envisages that for two possible forms of non-linearity, the PSO dynamics is stable for α^{l}_{t-1} in [0, 0.013]. Computer simulation of the PSO algorithm confirmed the above results.

Acknowledgements

The authors would like to express their gratitude towards Prof. Amit Konar of ETCE Department, Jadavpur University, under whose able guidance this research was carried out.

References

[1] V.Kadirkamanathan, K.Selvarajah, P.J.Fleming, "Stability analysis of the particle dynamics in particle swarm optimizer," IEEE Trans. Evol. Comput., vol.10, no.3, pp. 245-255, Jun. 2006.

[2] R. C. Eberhart and J. Kennedy, "A new optimizer using particle swarm theory," in Proc. 6th Int. Symp. Micromachine Human Sci., vol. 1, Mar. 1995, pp. 39-43.

[3] R. C. Eberhart and Y. Shi, " Comparison between genetic algorithms and particle swarm optimization," in proc. 7th Conf. Evol. Program., vol. 1447, Mar. 1998, pp. 611-616.

[4] Y. Shi and R. C. Eberhart, "Empirical study of particle swarm optimization" Proc.IEEE Congr.Evol. Comput., 1999, pp1945-1950.

[5] R. Mendes, J. Kennedy, and J. Neves, "The fully informed particle swarm: Simpler, may be better," IEEE Trans. Evol. Comput., vol 8, no.3, pp 204-210, Jun. 2004.

[6] G. Ciuprina, D. Ioan, and I. Munteanu, "Use of intelligent particle swarm optimization in electromagnetics," IEEE Trans. Magn., vol. 38, no. 2, pp. 1037-1040, Mar. 2002.

[7] M. Wachowiak, R.Smolikova, Y. Zheng, J. Zurada, and A. Elmaghraby, "An approach to multimodal biomedical image registration utilizing particle swarm optimization," IEEE Trans. Evol. Comput., vol.8, no.3, pp. 289-301, Jun. 2004.

[8] L. Messerschmidt and A. Engelbrecht, "Learning to play games using a PSO-based competitive learning approach," IEEE Trans. Evol. Comput., vol.8, no.3, pp. 280-288, Jun. 2004.

[9] A. Ratnaweera, S. Halgamuge, and H. Watson, "Self-organizing hierarchical particle swarm optimizer with time-varying acceleration coefficients," IEEE Trans. Evol. Comput., vol.8, no.3, pp. 240-255, Jun. 2004.

[10] C. A. C. Coello, G. Pulido, and M. Lechuga, "Handling multiple objectives with particle swarm optimization," IEEE Trans. Evol. Comput., vol.8, no.3, pp. 256-279, Jun. 2004.

[11] R. C. Eberhart and X. Hu, "Multiobjective optimization using dynamic neighborhood particle swarm optimization," in Proc.IEEE Congr. Evol. Comput., May 2002, pp 1677-1681.

[12] K. E. Parsopouls and M. N. Vrahatis, "Particle swarm optimization method in multi objective problems, "in proc. ACM Symp. Appl. Comput. Evol. Comput., Madrid, Spain, May 2002, pp. 603-607.

[13] R. C. Eberhart and Y. Shi, "Parameter selection in particle swarm optimization," in Proc. 7th Conf. Evol. Program., vol. 1447, Mar. 1998, pp. 591-600.